

A Numerical Study on the Seismic Response of Circular CFST Column-Beam Exterior Joint with Split Bolt Assembly



P. U. Sreeshma and K. P. Beena

Abstract The concrete-filled steel tube (CFST) is a composite member consisting of a steel tube and concrete infill. CFST combines the advantages of both steel and concrete member as they are placed concentrically. Circular CFST columns show better performance compared to square one, as they provide more confinement to concrete infill. But the application of circular CFST columns is limited, due to the difficulties in assembling the connection. Split bolt assembly avoids the complications in the circular CFST column connections and improves the efficiency of the joint compared to straight bolt assembly. Split bolt assembly allows the intersection of through bolts at the same level. In this work, the seismic response of an exterior semi-rigid stiffened extended endplate connection between circular CFST column and I-beam with split bolt assembly is studied under displacement-controlled cyclic loading. The numerical study was conducted to investigate the influence of axial load level and split bolt angle on the joint behaviour. Initial stiffness of joint increases with increase in axial load level but has negligible effect on moment capacity of the joint.

Keywords CFST column · Split bolt assembly · Semi-rigid · Extended endplate · Cyclic loading · Axial load level

1 Introduction

The concrete-filled steel tube (CFST) is a composite member consisting of a steel tube filled with concrete. In the last few decades, CFST columns have been widely used in engineering applications because of their excellent structural performance obtained

P. U. Sreeshma (✉) · K. P. Beena
Trivandrum, India
e-mail: sreeshmapu999@gmail.com

K. P. Beena
e-mail: beenakp@cet.ac.in

from the positioning of steel tube and concrete core concentrically. The steel tube provides confinement [2] and thus increases the strength and stiffness of concrete core, and the concrete in turn reduces the possibility of local buckling of tube wall. Steel tube acts as a formwork, thus increasing the speed of construction. The provision of steel tube provides the benefits of both longitudinal reinforcement and transverse confinement; hence, the traditional longitudinal and transverse reinforcement can be avoided. Circular CFST columns have better performance compared to square CFST columns as the circular tube provides more confinement to concrete core. In square- and rectangular-shaped tubes, due to the weak confining effect the concrete core and the steel tube do not keep in contact with each other during the ultimate loading stage. In the case of circular sections, local buckling is not likely to occur due to this strong confining action [3]. The application of CFST circular columns is limited even though it has a better performance compared to square CFST columns due to the practical difficulties faced in connecting the circular CFST column to beams.

Seismic response of a CFST structure depends upon the beam-column connections as they are critical elements in transferring beam loads to column and ensuring structural safety [14]. The connection between CFST column and steel beam can be exterior or interior connections. In exterior connection steel beam is directly attached to the skin of the steel tube and hence experiences heavy distortion in the tube wall at the connected region [5]. High weld stresses are developed in the welded connection during a seismic event and lead to brittle failure. Welded connections are widely used for exterior joint. In interior connections, the steel beam is allowed to pass through the CFST column by cutting an opening in the tube wall [9]. This connection provides interference with the concrete and is difficult to construct in the field.

Rigid connections are completely welded connections, which is effective in transferring bending moment, shear force and axial load between beam and CFST column [8]. But the relative rotation between beam and column is negligible. Rigid connections are expensive to make due to the inclusion of many stiffening elements and need of heavy welding. To avoid extensive welding and to improve the performance of joint, connections using high-strength bolts are used in CFST structures [6]. A semi-rigid endplate connection helps to avoid weld failure and requires only shop welding and on site bolting works [7]. The semi-rigid connection with an extended reinforcement bar or bolts helps to transmit the stresses to concrete core. As an alternative solution to the problems associated with through beam connections, through bolted connections are also used. Through bolted connection allows a bolt rod to pass through the CFST column and act as a tie rod, which increases the concrete confinement and making it to actively participate in lateral stability [11]. It is difficult to get the grip between steel tube and bolt head while providing straight bolt assembly in a circular CFST column. One solution to avoid the technological difficulties is the provision of curved endplates [12]. Split bolt assembly is used to provide through bolts in circular CFST column connections. This will allow the diametrical intersection of bolts at the same level. Stiffeners are provided where large load-carrying capacity of the joint is required, and it also helps to shift the location of plastic hinge away from the column face and reduces stress concentration at the column face.

From an extensive review of the available literature on CFST beam-column joint, it was found that fewer studies are so far reported in the area of circular CFST beam-column joint compared to square one. Studies on split bolt assembly in circular CFST columns are very rare in the literature. Since circular CFST columns with split bolt assembly improve the structural seismic performance significantly, an extensive research is needed in this field.

The main objective of the study is to investigate the seismic behaviour and failure modes of a stiffened extended curved endplate connection between circular CFST column and steel beam with split bolt assembly. The seismic behaviour of this connection depends on many parameters such as material, geometry and loading. It is difficult to consider all parameters by experiment. Hence, in this study the commercial software ABAQUS is used to simulate the seismic behaviour of I-beams in through bolted beam-column connections and to calibrate this behaviour with experimental results available in the literature. The study focuses on the influence of axial load level of CFST column and angle of split bolt assembly on the joint behaviour.

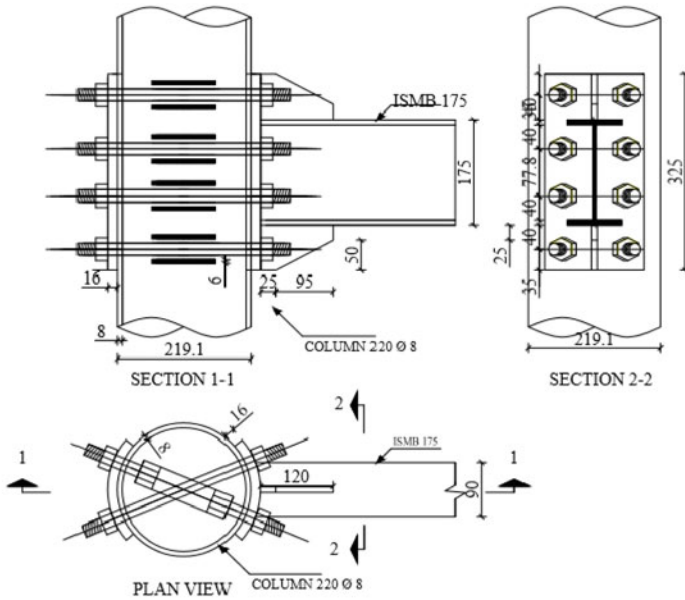
2 Finite Element Model

A finite element model was developed using ABAQUS software for the through bolted curved extended endplate connection between circular CFST column and steel beam with vertical stiffeners and split bolt assembly. The details of joint are given in Table 1.

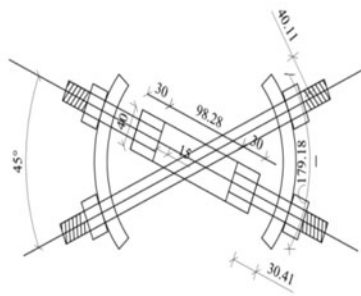
The joint shown in Fig. 1 consists of a circular tube of 220 mm diameter and 8 mm thickness with 300 Grade and beam ISMB 175 with 250 Grade. The beam was welded to 16 mm thick curved extended end plate. 10 mm thick triangular stiffeners with 120 mm length were provided above and below the top and bottom flanges. 20 mm rod 8.8 Grade High Strength Friction Grip is used to form through bolts.

Table 1 Details of joint

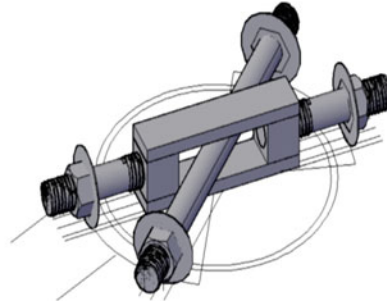
Component	Dimensions	Length (mm)	Thickness (mm)
Steel tube	220 mm dia	1500	8
Concrete core	204 mm dia	1500	–
I-beam	ISMB175	800	$t_w = 5.5, t_f = 8.6$
End plate	158 mm × 325 mm	–	16
Stiffener	120 mm × 75 mm	–	10
Through bolt	M20	Shank length = 252	–



(a) Details of specimen.



(b) Details of split bolt assembly.



(c) Split bolt assembly (3D view).

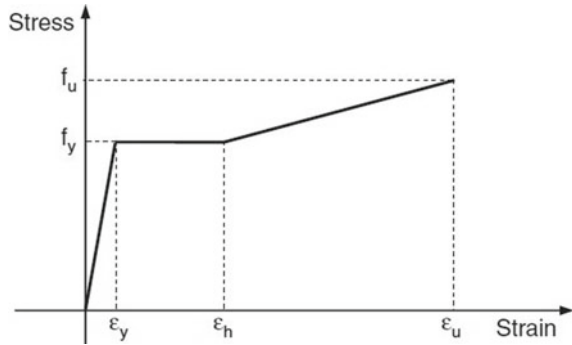
Fig. 1 Joint details [1]

2.1 Material Model

2.1.1 Material Model of Steel

The elastic–plastic model was used to describe the behaviour of the steel. Tri-linear stress–strain curve proposed by Zhong et al. [13] as shown in Fig. 2 was used for tube, end plate, beam, stiffener and bolt. The “plastic” option available in ABAQUS allows to use a multi-linear stress–strain curve. The first part of the tri-linear curve

Fig. 2 Stress–strain model of steel [13]

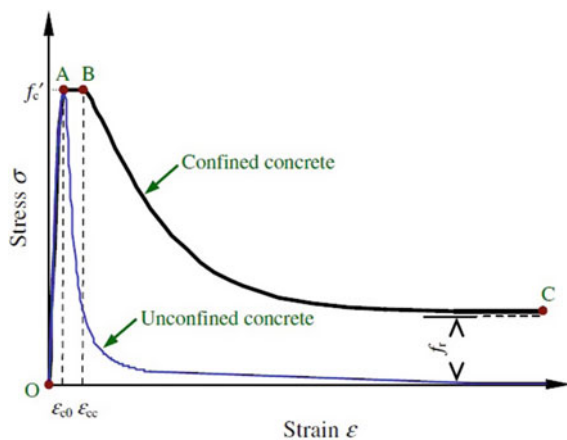


represents the elastic curve up to the proportionality limit stress defined by Young’s modulus and Poisson’s ratio. Poisson’s ratio is taken as 0.3 and Young’s modulus as 200 GPa. After the onset of yielding, steel is assumed to be fully plastic until strain hardening.

2.1.2 Material Model of Concrete

The confined concrete model proposed by Zhong et al. [13] was adopted in the FE analysis. Figure 3 shows the uniaxial stress–strain curve used to define the parameters required in “concrete damaged plasticity” model available in ABAQUS. Uniaxial tensile response was assumed to be linear until the tensile strength of concrete was reached and was taken as 0.1 times the cylinder compressive strength. At this point, plastic strain was zero.

Fig. 3 Stress–strain model for confined concrete [13]

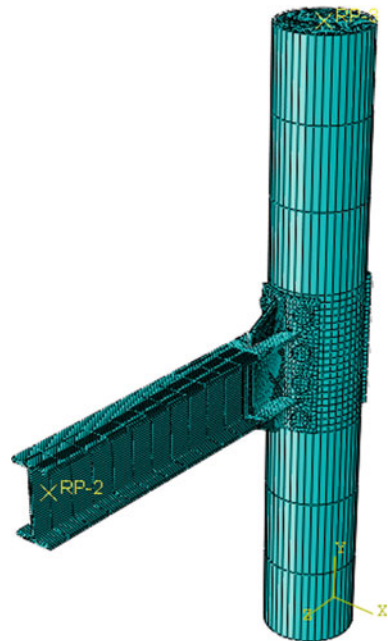


2.2 Geometric Model

In the FE model, three-dimensional 8-node linear brick element with reduced integration and hourglass control (C3D8R) was used for all the components of the joint. This element is not susceptible to shear locking, which makes the model stiffer. Structural meshing technique was used to have a proper element shape [10].

The different parts were assembled together by contact relations and constraints between the surfaces to form the analytical model of CFST beam-column joint. The interaction between the different surfaces among steel parts and concrete core was given through the “contact pair” algorithm, where the surfaces can contact and separate each other but are not allowed to penetrate. The curved surfaces which come into contact including the steel tube inside surface to concrete core outside surface, endplate to steel tube outside surface, bolt head to endplate, bolt shank to bolt holes on the steel tube, bolt shank to bolt holes on the endplate and bolt shank to concrete core were defined with hard contact and coulomb friction model in the normal and tangential directions [4]. The coefficient of friction between the two surfaces in the model has moderate effect on the joint behaviour and was taken as 0.2 for better convergence. The welded connection between beam and end plate, beam and stiffener, stiffener and endplate are simulated using the “tie” constraint, which allows to couple all degrees of freedom for the welded components. A schematic view of the FE model developed is shown in Fig. 4.

Fig. 4 Finite element model of joint



For boundary conditions, all three rotational degrees of freedom were allowed at both ends of the column. The translational degrees of freedom except the vertical displacement were restrained at the loading end of the column. All the three translational degrees of freedom were restrained at the other end of the column.

A nonlinear quasi-static analysis of the joint was performed. Material, geometrical and boundary nonlinearities are considered in the analysis. In order to reflect the actual loading condition, three loading steps were adopted in the FE analysis to apply different loads including bolt pretension force, column axial load and beam load. Bolt pretension force of 100 kN was applied firstly at the centre of the bolt. Second step was to apply a constant axial load equal to 15% of the axial load-carrying capacity of the CFST column at the top of the column through the reference point (RP-3 in Fig. 4) of the “rigid body constraint”. In the third step, displacement-controlled cyclic load was applied at a distance of 50 mm from the tip of the beam through a reference point (RP-2 in Fig. 4) using ANSI/AISC 2002 loading protocol as given in Fig. 5. This reference point acts as a loading plate as it is connected to the slave nodes in the beam at a section through the “multipoint constraint” option available in ABAQUS.

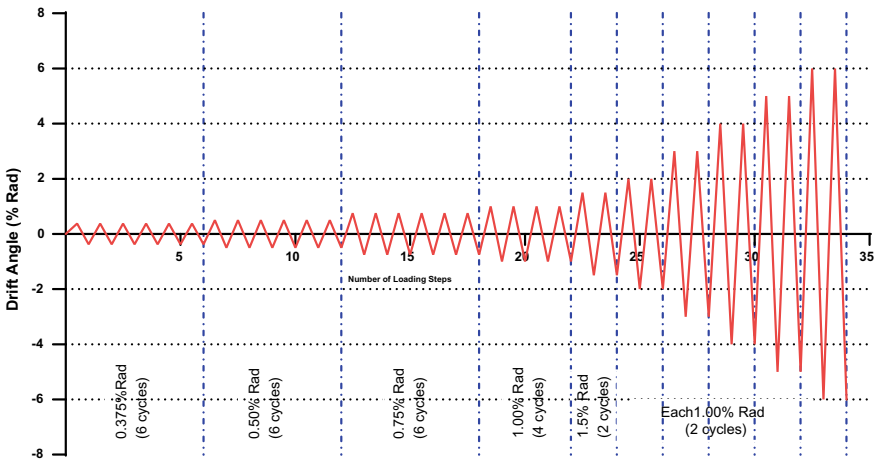
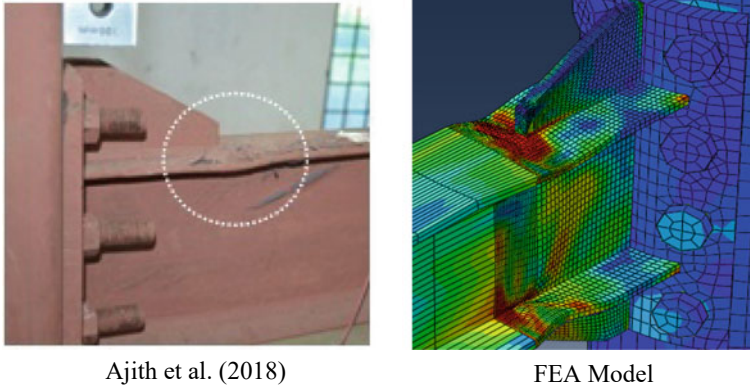


Fig. 5 Loading protocol



Ajith et al. (2018)

FEA Model

Fig. 6 Failure modes of joint

3 Results and Discussion

3.1 Failure Mode

The deformed shapes observed in the experiment by [1] and numerical studies are compared in Fig. 6. The joint failed in strong joint, strong column–weak beam mode. As expected severe local buckling occurs in the flanges and web of the beam at the end of vertical stiffener, indicating the formation of an obvious plastic hinge. From the experimental and numerical results, the failure modes of the joint are ductile in nature. It can be concluded that the energy is dissipated mainly through beam flexural yielding and subsequent buckling in both experimental and numerical results.

3.2 Moment-Rotation Relationship

The hysteresis loop obtained from numerical study using moment and angular rotation is shown in Fig. 7. Moment at the column face was calculated by multiplying the force at the tip of the beam with distance between the column face and loading line. The total rotation of the joint was contributed by beam, column and panel zone. But the major contribution for joint rotation might be from beam as the design philosophy of strong joint, strong column and weak beam was followed. The curve showed good hysteresis behaviour with no pinching effect. The hysteresis curve obtained was plumb in shape with increase in loop area indicating that the joint has good energy dissipation capacity.

As it is difficult to validate a hysteresis curve, each maximum load points in a loading cycle was used to construct a moment-rotation envelope curve for the joint as shown in Fig. 8. Peak minimum rotation observed was greater than 0.04 rad, which

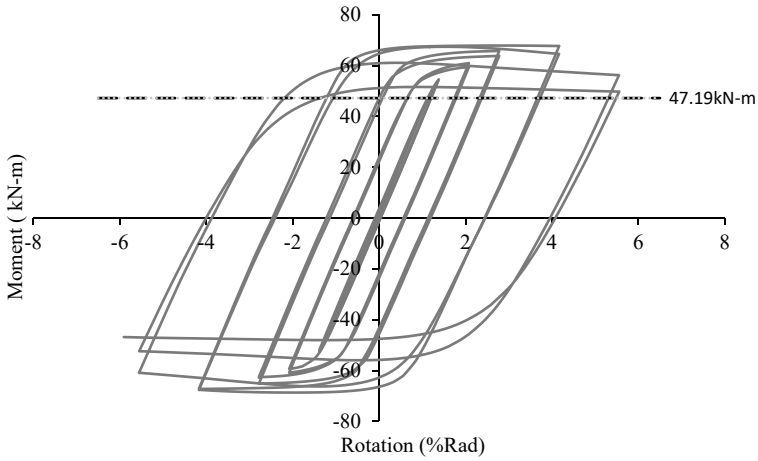


Fig. 7 Moment-rotation hysteresis curve

satisfies the guidelines provided by AISC 341-10 for composite special moment resisting frame. In Table 2, a comparison between numerical and experimental data for moment capacities and initial stiffness is shown. Numerical results are overestimated. But the shapes of curves obtained in both cases are similar. The comparison indicates that the current FE model has reasonable prediction accuracy and can be used for further parametric study.

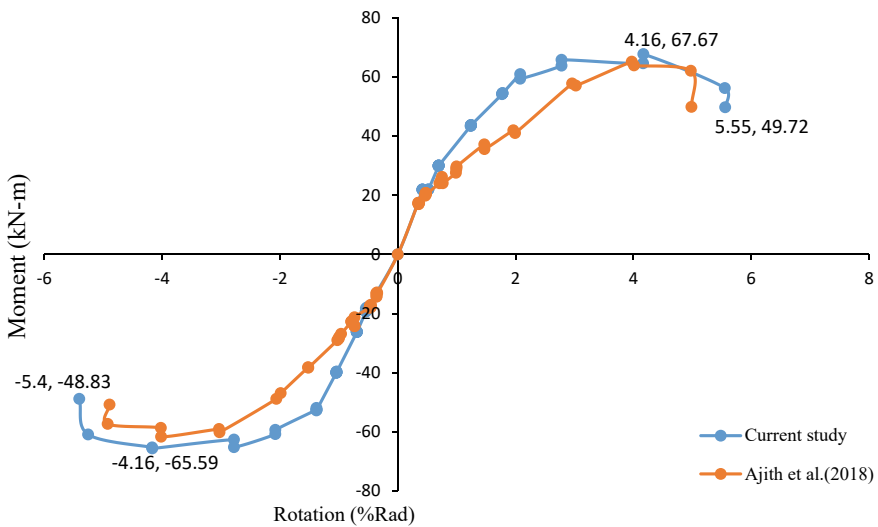


Fig. 8 Moment-rotation envelope curve

Table 2 Validation of results

	M_u (kN-m)		$\theta_{r,u}$ (rad)		S_{ini} (kN-m/rad)	
	H	S	H	S	H	S
FEA	67.66	65.59	4.16	4.16	44.88	35.00
[1]	65.12	61.66	3.97	4.04	44.8	34.09

Note: M_u = ultimate moment;; $\theta_{r,u}$ = rotation at ultimate moment; S_{ini} = initial stiffness; H = hogging; S = sagging

3.3 Effect of Axial Load Level

The current FE model was used to study the influence of axial load level in the moment capacity and initial stiffness of the joint. Axial load level of CFST column can be defined as,

$$n = N/N_u, \tag{1}$$

where N and N_u are the axial compressive load and ultimate axial compressive load applied to CFST column, respectively.

To study the effect of axial load level on joint behaviour, models were analysed for axial load levels of 0.05, 0.15 and 0.25. The moment-rotation curves obtained from the analysis are shown in Fig. 9. The initial stiffness of the connection increases with increase in axial load level, but has negligible effect on the ultimate moment capacity of the joint. The initial stiffness was enhanced by 27% in positive and negative displacement when the axial load level increases.

3.4 Effect of Angle of Split Bolt Assembly

A split bolt assembly consists of two through bolts passing diametrically and intersect each other at the same level. The model which is validated has a split bolt assembly with 45° angle between the bolts. Finite element model of the bolted joint with angle of split bolt assembly 35°, 45° and 55° is developed for investigating the effect of the bolt angle on the behaviour of joint. Moment-rotation envelopes are developed for these values of angle of split bolt assembly which is shown in Fig. 10. It is observed that, increase in the angle of split bolt assembly enhances both initial stiffness and ultimate moment capacity of the joint. This is because when the angle of split bolt assembly increases, pitch of the bolts also increases so that the portion of the panel zone confined by the split bolt assembly also increases. That will result in a strong panel zone with increased moment capacity and stiffness of the joint. It was found that as the angle of split bolt assembly increases, moment capacity and initial stiffness of the joint were found to be enhanced by 12 and 39% in positive and negative displacement.

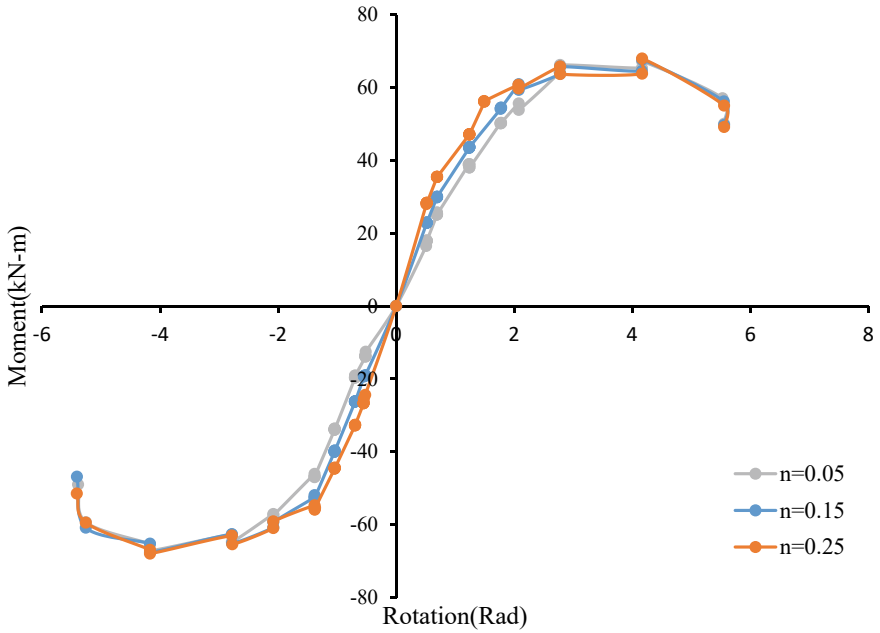


Fig. 9 Effect of axial load level

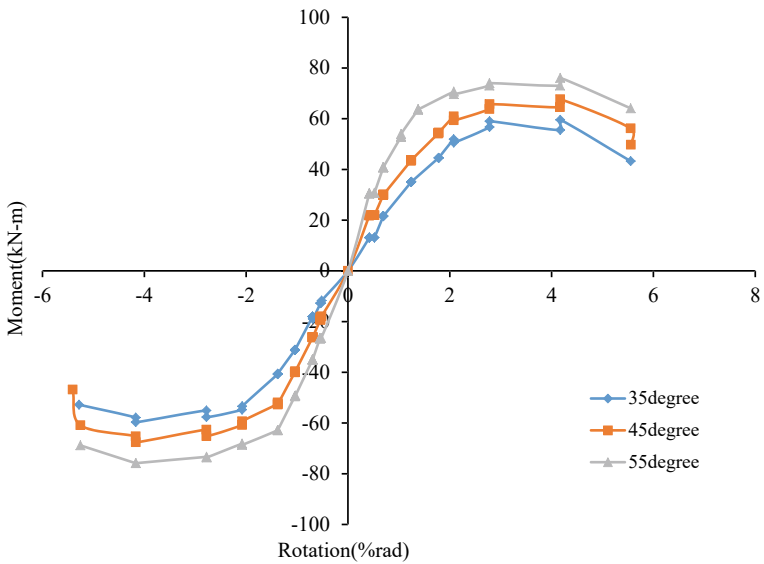


Fig. 10 Effect of angle of split bolt assembly

4 Summary and Conclusions

The behaviour of a stiffened curved extended endplate connection between circular CFST column and I-beam with split bolt assembly under displacement-controlled cyclic load is explored in this study. The FE model of the joint was generated using a confined stress–strain model of concrete and a tri-linear model of steel. The accuracy of model was verified using the experimental results of Ajith et al. [1] in terms of the moment versus rotation relationship and deformed shape. The effect of axial load level and angle of split bolt assembly on the joint behaviour was studied.

The principal conclusions of the present work on the behaviour of CFST beam-column exterior joint are stated below:

1. Nonlinear FEA can be used to predict the ultimate strength and failure modes of circular CFST beam-column exterior joint with sufficient accuracy.
2. The FEA model showed a flexural failure of beam which satisfied the design criteria of strong joint, strong column and weak beam.
3. The total rotation of the joint observed was greater than 0.04 rad in both positive and negative cycle which satisfy the guideline provided by AISC 341-10 for composite special moment resisting frame.
4. Moment versus rotation curve shows a stable behaviour with increase in loop area, indicating the ductile behaviour of joint.
5. The initial stiffness of the joint was found to increase by 27% for positive and negative displacement when the axial load level increases, but it has negligible effect on the moment capacity of the joint.
6. Moment capacity and initial stiffness of the joint were found to be increased by 12 and 39% in positive and negative displacement with increase in angle of split bolt assembly.

References

1. Ajith MS, Beena KP, Sheela S (2018) Comparative study on hysteretic performance of semi through connections in CFT beam-column joint. In: International conference on infrastructure development: issues, innovations and way forward (ICID), pp 81–89
2. Hoang V-L, Jaspert J-P, Demonceau J-F (2015) Extended endplate to concrete filled rectangular column joint using long bolts. *J Constr Steel Res* 113:156–168
3. Hu HT, Huang CS, Chen ZL (2005) Finite element analysis of CFT columns subjected to an axial compressive force and bending moment in combination. *J Constr Steel Res* 61:1692–1712
4. Jingfeng W, Zhang N (2017) Performance of circular CFST column to steel beam joints with blind bolts. *J Constr Steel Res* 82:33–47
5. Kharoob OF, Ghazy MF, Yossef NM (2017) Behavior of beam- high performance fiber reinforced CFST column joint. *Thin-Walled Struct* 113:217–227
6. Lee J, Goldsworthy HM, Gad EF (2010) Blind bolted T-stub connections to unfilled hollow section columns in low rise structures. *J Constr Steel Res* 66(8–9):981–992
7. Li X, Xiao Y, Wu YT (2009) Seismic behavior of exterior connections with steel beams bolted to CFT columns. *J Constr Steel Res* 65:1438–1446

8. Schneider S, Alostaz Y (1998) Experimental behaviour of connections to concrete-filled steel tubes. *J Constr Steel Res* 453:321–352
9. Sheet IS, Umaranim G, MacRae GA (2013) Experimental investigation of CFT column to steel beam connections under cyclic loading. *J Constr Steel Res* 86:167–182
10. Thai H-T, Vo TP, Nguyen T-K, Pham CH (2017) Explicit simulation of bolted endplate composite beam-to-CFST column connections. *Thin-Walled Struct* 119:749–759
11. Wu L-Y, Chung L-L, Tsai S-F, Lu C-F, Huang G-L (2007) Seismic behavior of bidirectional bolted connections for CFT columns and H- beams. *Eng Struct* 29:395–407
12. Yao H, Goldsworthy H, Gad E (2008) Experimental and numerical investigation of the tensile behavior of blind-bolted T-stub connections to concrete-filled circular columns. *J Struct Eng* 134(2):198–208
13. Zhong T, Wang Z-B, Qing Y (2013) Finite element modelling of concrete-filled steel stub columns under axial compression. *J Constr Steel Res* 89:121–131
14. Zhong T, Wei L, Bo-Lin S, Lin-Hai H (2017) Behaviour of bolted end-plate connections to concrete-filled steel column. *J Constr Steel Res* 134:194–208